# Modeling and Experimental Verification of the Power Transfer and Thermal Characteristics of Piezoelectric Transformers Subjected to Combined Mechanical and Electrical Loading

Safakcan Tuncdemir[1], William M. Bradley[*2]
[1]Solid State Ceramics Inc., Williamsport, Pennsylvania 17701,
[2]QorTek Inc., Williamsport, Pennsylvania 17701
*Corresponding author: 1965 Lycoming Creek Road, Williamsport, PA 17701, mbradley@qortek.com

**Abstract:** A piezoelectric transformer allows purely mechanical transfer and scaling of electrical energy via simultaneous utilization of both the direct and converse piezoelectric effects. This mechanical energy transfer enables a wide range of functional differences from typical magnetic-based electrical power transformers. Comparing to their electromagnetic counterparts, piezoelectric transformers are highly efficient and can have significantly high power density within reduced operating volumes. However, they need to be operated at resonance, which results in a complex non-linear system that requires significant design and analysis for effective system integration. In order to aid in the development of such high efficiency, high power throughput piezoelectric transformers we have developed a realistic COMSOL Multiphysics model and a range of experimental test setups for empirical verification. The model is capable of coupling both mechanical and electrical loads to the piezoelectric transformer, thus enabling examination of the thermal effects from the associated losses in the device. In this work, we are interested in the analysis of the piezoelectric devices at high power density and high frequencies, which will increase thermal loads generated by the device. Additionally, the model is capable of studying various environmental parameters such as dynamic electrical loading, mechanical and thermal effects from system packaging, and variations of input conditions.

**Keywords:** Piezoelectric, transformer, high efficiency energy transfer, high power density, coupled physics, thermal analysis, electrical analysis.

## 1. Introduction

Since the first piezoelectric transformer (PT) was introduced by Rosen in 1956, many designs have been revealed for various purposes [1-4]. PTs are highly efficient and can have significantly high power densities. They can also be easily integrated as circuit elements since they are free from electromagnetic fields and the related emission and susceptibility problems associated with their magnetic counterparts. PTs are also commonly designed to maintain very low form-factors, which is an additional benefit to integration in modern electronics systems. There has been a growing interest on the analysis of PTs in the last decade due to the rapid expansion of portable and miniaturized electronic equipment industries where PTs fit perfectly based on their abovementioned merits. However, despite the superior features and small scale, the inherent losses and demanding drive circuitry prevents wider utilization of these devices [4].

Piezoelectric devices are typically driven with device-specific input signals for optimum performance. Moreover, piezoelectric material properties, and hence their overall device characteristics, including the optimum driving point, are greatly affected by any change in boundary conditions; such as by fluctuating external load, temperature rise or mechanical clamping. Therefore maintaining the optimum performance for desired output power, efficiency and voltage gain levels under dynamic thermal, electrical and mechanical loading is extremely difficult.

In addition to the load dependence and demanding driving conditions, inherent loss of piezoelectric materials is another crucial problem that hinders the further employment of PTs in a wider scope of applications. Inherent losses in the material causes heat generation, which raises the device temperature. Temperature determines the operational limit as the ferroelectric material of the PT must be operated below the Curie Temperature ($T_C$) to prevent permanent damage to the device. Thermal stress, which is another effect of temperature change, may lead to stress based failures. Even with the temperature below the level for mechanical failure and $T_C$, slight changes affect the device performance as well, as it shifts the optimum operating point and increases the demand for intelligent control.

Therefore, a fully coupled, realistic device model is required to analyze PTs in service conditions that include thermal, electrical, and mechanical loads. COMSOL Multiphysics has enabled us to begin development of a piezoelectric device model which enables analysis of these simultaneously interacting physics. This device model can then be integrated into the iterative design process, thus alleviating the need to fabricate individual design revisions.

In this work, we present an effective PT model in COMSOL, which is in close agreement with comparable experimental test data of electrical and thermal characteristics of a Rosen type PT. We provide comparisons of COMSOL to experimental data and a lumped-parameter equivalent circuit model by studying voltage gain, resonant frequency, and input impedance, as well as thermal distribution.

## 2. Operating Principle of Rosen Type Piezoelectric Transformer

Piezoelectric materials develop a charge when mechanically stressed (the direct piezoelectric effect) and develop a strain upon the application of an electric field (the converse piezoelectric effect). Piezoelectric transformers combine both the direct and converse piezoelectric effects to convert AC voltage at the primary to a proportional voltage at the secondary.

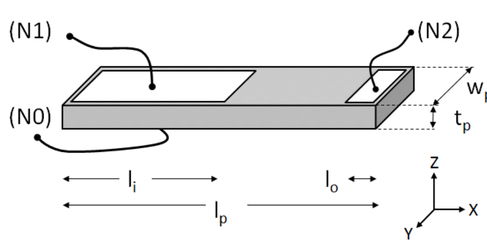


**Figure 1:** Diagram of Rosen Type Piezoelectric Transformer

In this work, we report experimental verification of a COMSOL Multiphysics model of a Rosen type transformer. A basic sketch of the single layer Rosen type PT with its input (N1-N0) and output electrodes (N2-N0) is shown in **Figure 1**. The left half of the ceramic material is poled in thickness direction (Z-poled) while the other half is poled in the length direction (X-poled). When an alternating sinusoidal voltage is applied to the Z-poled half of the ceramic at the resonant frequency, a continual longitudinal vibration occurs. The vibrations are mechanically coupled to the x-poled region where they induce a potential difference between N2-N0. That is, the input region behaves like a piezoelectric actuator (the converse piezoelectric effect), and the output region behaves like a piezoelectric transducer (the direct piezoelectric effect).

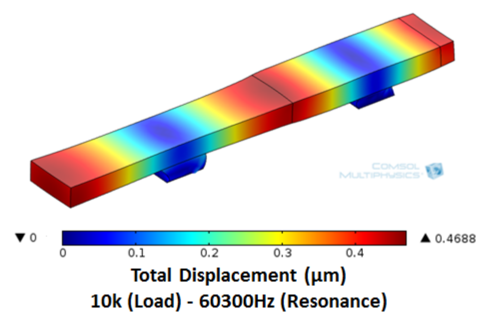


**Figure 2:** Total Displacement at Second Longitudinal Resonance Mode

PTs are operated at their fundamental modes in order to benefit from the maxim strains exhibited due to resonance. The associated resonance mode shape changes depending on the device geometry and excitation frequency. The second longitudinal resonance mode will be employed in our study due the use of the bar shaped geometry. **Figure 2** shows the displacement profile of the bar at resonance, where two nodal (no displacement) regions appear around one fourth of the total length from each side. **Table 1** details the geometric parameters of the PT used in the model as well as the physical test device. The device dimensions are also indicated in **Figure 1**.

**Table 1:** Geometric Parameters of the Piezoelectric Transformer

| Parameters | Value |
|---|---|
| $l_p$ | 53 mm |
| $l_i$ | 26.65 mm |
| $l_o$ | 2 mm |
| $t_p$ | 2.59 mm |
| $w_p$ | 7.4 mm |

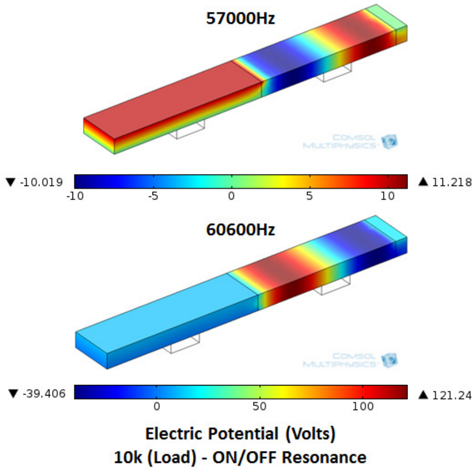


**Figure 3:** Voltage Distribution of PT at Resonance (Bottom) and Off Resonance (Top)

**Figure 3** shows the voltage distribution of the transformer during operation (**Top**, off-resonance; **Bottom,** resonance). A 10V input voltage is seen on the primary side of the transformer while operated at off-resonance. The amplified output voltage due to the maximized stress at resonance can be seen in the bottom diagram.

## 3. Use of COMSOL Multiphysics

Compared to their electromagnetic counterparts, piezoelectric transformers have higher power density with high conversion efficiencies. However, superior power characteristics of PT are strictly dependent on following three main conditions:

1. *Maintaining the optimum driving conditions, such as phase and resonance frequency tracking.*
2. *Keeping heat dissipation under control to limit thermal build up.*
3. *Eliminating the effect of changing load conditions.*

There are many studies in literature which report different techniques to address these problems for enhancing the output characteristics of PT. Despite the differences in the methods to design effective PTs, the need for an extensive yet simple-to-use model is common and fundamental in previous studies.

PT characteristics depend heavily on the interactions between their electrical, mechanical, and thermal conditions, especially when operated at high power, high load and in thermally isolated cases. Therefore, an extensive PT model should include coupling of these associated physics. Due to COMSOL's modular Multiphysics interface, we have been able to effectively model a Rosen type transformer. **Figure 3** shows the top level flow chart of the COMSOL model built for the feasibility analysis. In the model, a piezoelectric transformer is coupled with input/output circuit and operates within an air chamber which functions as heat sink. Additionally, silicone rubber base supports are used to hold the device, and are included in the thermal analysis.

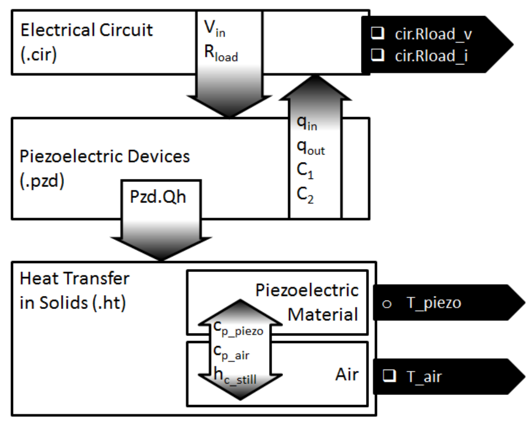


**Figure 4:** Logical Diagram of COMSOL Model Physics

As shown in **Figure 4**, the Piezoelectric Devices module accepts drive conditions and circuit parameters from the Electrical Circuit module. The input and output impedance of piezoelectric device changes based upon on the excitation frequency of the drive circuit. Additionally, the charge generated at output fluctuates significantly across such conditions (see **Figure 3, bottom**). These effects are reflected back to the Electrical Circuit module through which the electrical characteristics of total PT model are measured.

Thermal characteristics of the model are obtained by using the Heat Transfer in Solids module of COMSOL. The model assumes the internal losses in the piezoelectric material as the sole heat source for the complete system. Heat transfer within the transformer body and towards the surrounding air is calculated inside this module. Finally, the thermal profiles of the materials are obtained from the results of this sequence.

### 3.1 Governing Equations

In order to have better understanding of the effect of material properties and the coupled physics, we identify the equations which are the basis for the finite element analysis below. The constitutive equations that describe the piezoelectric effect can be written in the stress-charge form as in *eq.1* and *eq.2*, where $T$, $S$, $E$ and $D$ are the mechanical stress, strain, electric field and the electric displacement, respectively. In the equations (*eq.1*, *eq.2*) coefficients $e$, $c^E$ and $\varepsilon^S$ are the piezoelectric coefficient, elastic compliance coefficient under constant electric field and the permittivity under constant stress, respectively.

$$T_i = c_{ij}^E S_j - e_{mi} E_m \quad (1)$$
$$D_i = e_{mi} S_j + \varepsilon_{ik}^S E_k \quad (2)$$

A new piezoelectric material model was generated in stress-charge form based on the factory provided material matrices ($c_{ij}^E, e_{mi}, \varepsilon_{ik}^S$ ) and isotropic properties ($\rho$ −density, $\kappa$ −thermal conductivity and $C_p$ −thermal capacitance) of the test sample.

Heat generation in piezoelectric materials and thus in the PT is due to the internal material losses, which are considered to have three components: dielectric, elastic and piezoelectric [6]. However, in this study we use only isotropic elastic ($\phi$) and dielectric loss factors ($\delta$) as 0.0006 and 0.004 respectively.

$$c^{E^*} = (1 - jtan(\phi))c^E \quad (3)$$
$$\varepsilon^{S^*} = (1 - jtan(\delta))\varepsilon^S \quad (4)$$

Heat source ($Q$) is the integrated heat generation of the piezoelectric material as defined by COMSOL (*pzd.Qh*). Generalized heat transfer is expressed by combining thermal conduction and the weak boundary conditions ($Q_{vh}$, $W_p$) as shown in *eq.5*.

$$\rho C_p \cdot \nabla T = \nabla \cdot (\kappa \nabla T) + Q + Q_{vh} + W_p \quad (5)$$

### 3.2 Boundary Conditions

The piezoelectric transformer is held by two rectangular rubber pieces from the nodal point as shown in **Figure 5**. The bottom of the rubber piece is mechanically fixed; however, since they are connected where there is no motion, there is minimum mechanical influence.

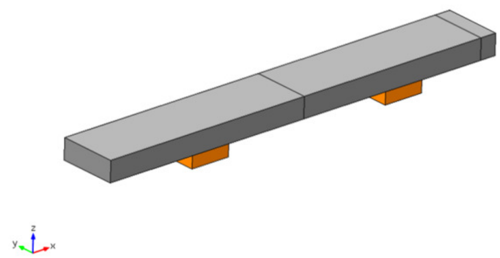

**Figure 5:** Rosen PT Model Geometry

The temperature of the base plate that contacts the rubber feet is fixed at ambient temperature ($T_{ambi}$). Outflow boundary conditions were defined for the outer boundary of air cavity.

The piezoelectric material's excitation signal is provided by an AC voltage source built into the Electrical Circuit module. An external load ($R_{load}$) is studied parametrically in the frequency spectrum in order to analyze the electrical load dependence of the PT. In addition to $R_{load}$, the effects of the probe impedance were introduced to further emulate the electrical test setup, as to improve the modeling results.

Additionally, in order to measure the current input to the transformer, the primary electrode is defined as a *Boundary Probe* with an *Inward Current Density* expression. If the probe result is integrated across the defined surface boundary, input current can be obtained.

$$I_{in} = \oint (pzd.nJ) dS \quad (6)$$

### 3.3 Meshing

The mesh view of the complete model is given in **Figure 6**. For our model the mesh was refined around the piezoelectric components, while optimized for solving time in the air domains.

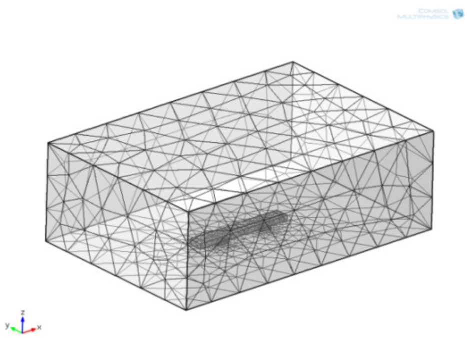

**Figure 6:** Meshing of Complete Model

## 4. Lumped-Parameter Electrical Circuit Modeling

The traditional method for electrical modeling of piezoelectric transformers is to implement a lumped-parameter equivalent circuit to represent the mechanical properties of the PT as an electrical dual of a spring mass damper. This has been well documented and validated as an effective equivalency [2-5]. The equivalent parameters were obtained with an HP4395 impedance analyzer with the output of the PT short circuited. This results in measured values for $C_m$, $L_m$, $R_m$, and $C_{in}$, the output capacitance $C_{out}$ is then measured with the input terminals shorted resulting in the complete circuit. **Figure 7** below depicts the equivalent circuit utilized in this study. The acquired equivalent circuit parameters are included in **Table 2**.

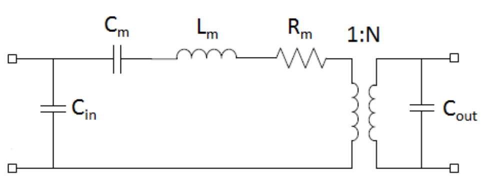


**Figure 7:** Piezoelectric Transformer Electrical Equivalent Circuit

For our comparison the equivalent circuit of the test device was measured via the described process and modeled with Linear Technologies SPICE software. This stage acted as a baseline comparison to traditional electrical design methods. The results of the SPICE electrical circuit modeling are provided along with the experimental and COMSOL model results in Section 6.

**Table 2:** Test Device Equivalent Circuit Parameters

| Equivalent Circuit Parameter | Value |
|---|---|
| $C_{in}$ | 787pF |
| $C_{out}$ | 8pF |
| $R_m$ | 30.6Ω |
| $C_m$ | 62pF |
| $L_m$ | 111.8mH |
| N | 8.2 |

## 5. Experimental Testing

In order to validate the results from the COMSOL model, we performed a range of experimental testing on a representative monolithic Rosen style PT (STEMInc. SMSTF68P10S9). The primary goal of this exercise has been to establish the validity of COMSOL Multiphysics for design development and device analysis of high complexity piezoelectric transformers. Therefore a logical first step has been to perform comparisons of COMSOL results with a less complex Rosen style PT. The preceding experimental efforts have been successfully targeted at such a validation.

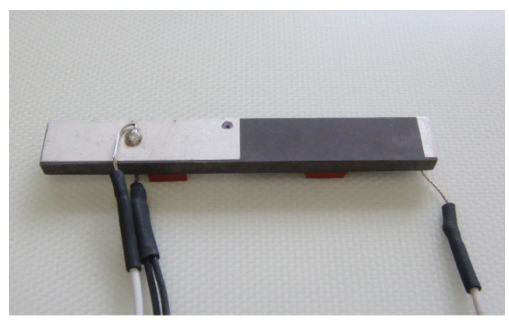

**Figure 8:** Rosen PT Device for Test

**Figure 8** above displays a sample of the test device included in the study. The device was driven with a 10V sinusoidal drive signal from a low output impedance linear amplifier at static frequency intervals. A Tektronix DPO7104 with Tektronix TCP0030 and Tektronix P6139A probes were used to acquire time domain peak current and voltage measurements of the test sample. This data allowed calculation of input impedance, and direct measurement of output voltage.

A second test was devised to measure the device's static temperature rise in air. For this test, a load of 10kΩ was preferred to allow substantial input current. This load resulted in a 164mW input power to the device with an electrical power transfer efficiency of approximately 87%. Under 10V sinusoidal drive at 60.3kHz (second longitudinal resonant frequency) maximum device temperature settles at 24.5°C which is 1.6°C higher than the ambient room temperature. A graphical representation of the results is shown in **Figure 12**.

## 6. Results

In order to verify the COMSOL model in the electrical domain we studied the input impedance and output voltage. Our electrical study includes the comparative analysis of COMSOL, SPICE and an experimental test. Additionally, for our thermal analysis, we compare the temperature distribution of a PT test device and the results from COMSOL.

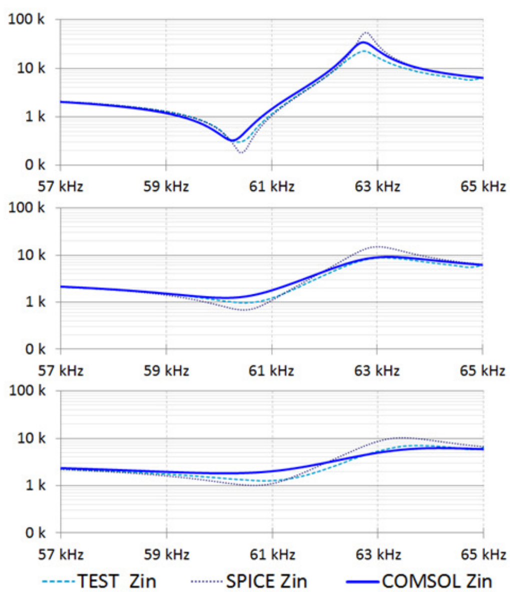


**Figure 9:** Modeling and Test Results - Zin (10kΩ, Top; 50kΩ, Middle; 100kΩ, Bottom)

**Figure 9** depicts the input impedance while **Figure 10** shows the peak output voltage for the range of load resistances (10kΩ, 50kΩ, and 100k) for the COMSOL Model, SPICE equivalent circuit model, and experimentally obtained test data. The resonant and anti-resonate frequencies can be identified by the peaks in the input impedance graphs. From these peaks, it can be seen that the COMSOL model adequately tracks the change in these frequencies due to the increased electrical loading.

Under the heaviest load condition (10kΩ) COMSOL had more accurate results when compared to the SPICE representation. The greatest deviation from the model and test occurred at high load resistances, this was largely attributed to the damping used within the model. The damping and loss used in the modeling were shown to be moderately high in terms of what is present in the physical sample, therefore a reevaluation of the damping mechanisms is planned for future efforts to further improve the overall model correlation.

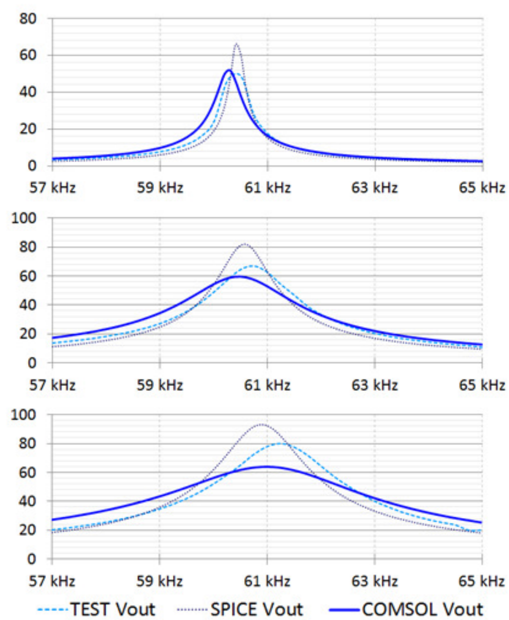


**Figure 10:** Modeling and Test Results - Vout (10kΩ, Top; 50kΩ, Middle; 100kΩ, Bottom)

In order to verify thermal behavior modeling with COMSOL, we measured temperature profile of the test sample with a FLIR i7 infrared camera and compared with COMSOL results. The top image in **Figure 11** shows the surface temperature of the top profile of the COMSOL model when driven with a 10V 60.3kHz AC source at ambient temperature. The bottom image displays an infrared camera reading of the test sample with similar drive conditions.

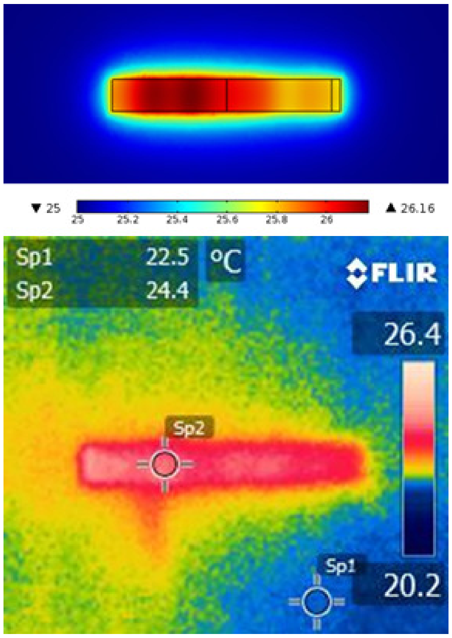


**Figure 11:** Surface Temperature Profile (Model, Top; Experimental, Bottom)

A final piece of the thermal analysis was to examine a temperature line profile across the center of the top surface of the PT, and compare this result to similar temperature profile data from the COMSOL modeling (**Figure 12**). While the profiles don't coincide, the overall values are in close proximity. It was also expected that the electrode material and electrical connections on the surface of the test device caused the respective dip in the test temperature in the 5 to 30mm range of the graph.

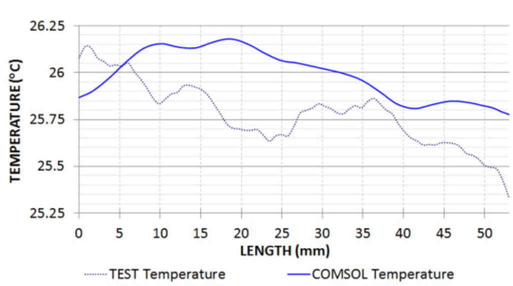


**Figure 12:** COMSOL Model and Test Results - Surface Line Temperature (10kΩ)

## 7. Conclusions

The results from this model validation effort have proven to be largely successful. The COMSOL model results display strong correlation with both the experimentally obtained test data as well as the electrical lumped-parameter modeling. These results adequately validate the COMSOL based PT model and enables a high level of confidence in utilizing COMSOL for development of higher complexity devices based on the same physics. While some discrepancies exist, most can be contributed to by obvious differences between the largely idealized COMSOL model and the physical test sample, such as lack of electrode material, connecting wires, and idealized poling as represented in the PT model. Further work on this study should include the thermal dependence of the piezoelectric material parameters and the inclusion of additional interacting physics, such as electric field and frequency dependence of complex losses.

## 8. References


1. C. A. Rosen, "Ceramic transformers and filters", *Electronic Comp. Symp.,* 205-211 (1956)

2. J. Yang, "Piezoelectric Transformer Structural Modeling – A Review", *IEEE Transactions on Ultrasonics, Ferroelectrics and Frequency Control*, Vol. 54, No. 6, 1154-1170 (2007).

3. S. Bronshtein, A Abramovitz, A, Bronshtein and I. Katz, "*A Method for Parameter Extraction of Piezoelectric Transformers*", Vol. 26, No. 11, 3395-3401 (2011)

4. E. L. Horsley, M. P. Foster and D. A Stone, "State-of-the-art Piezoelectric Transformer technology", *European Conference on Power Electronics and Applications,* 1-10 (2007)

5. Manh Cuong Do, *"Piezoelectric Transformer Integration Posibility in High Power Density Applications"*, Technische Universitat at Dresden (2008)

6. G. E. Martin, Dielectric, "Elastic and Piezoelectric Losses in Piezoelectric Materials", *Proc. Ultrasonics Symp*, 613-617 (1974)